ASTROPHYSICS AND SPACE SCIENCE LIBRARY 361

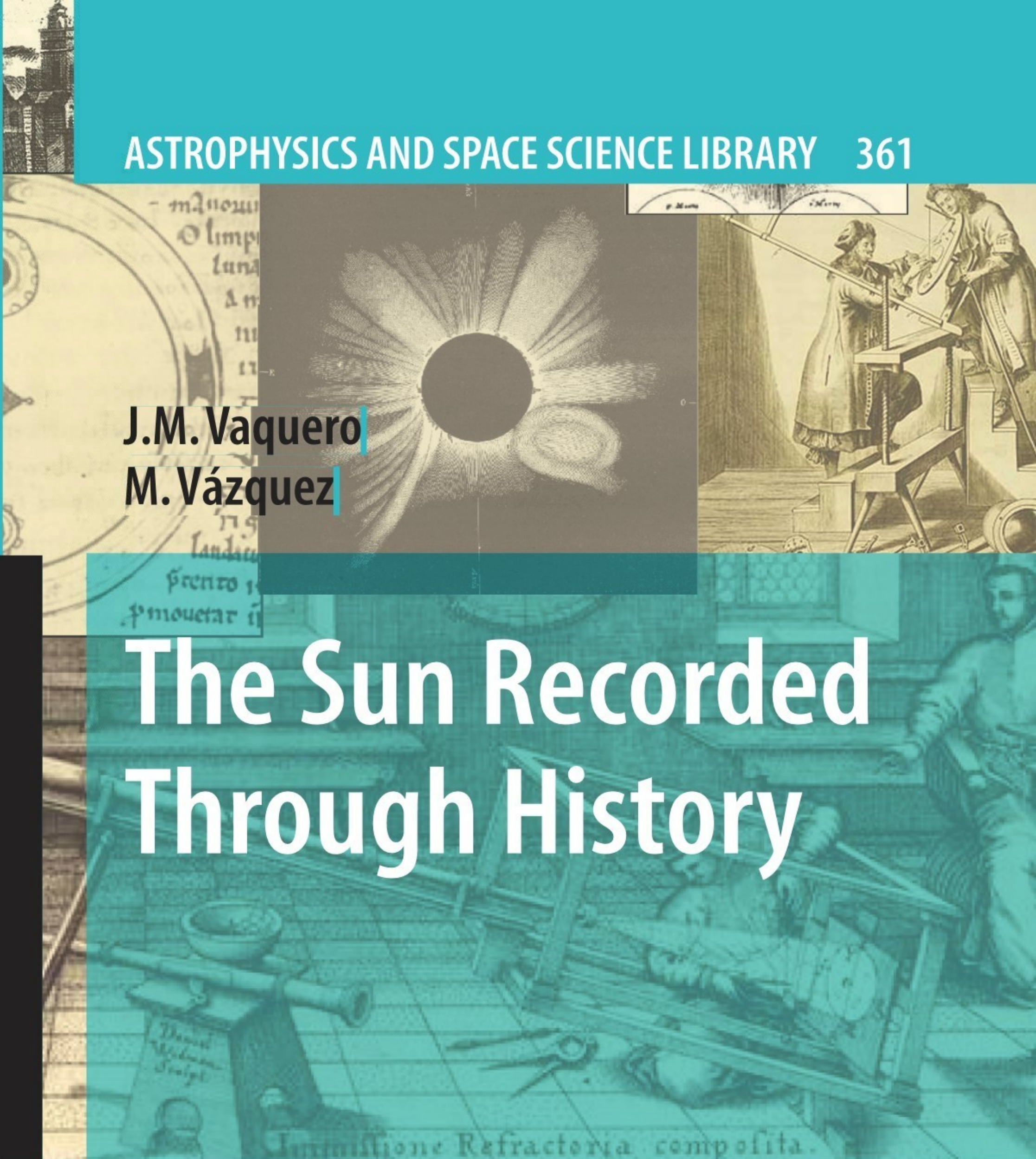


J.M. Vaquero
M. Vázquez

# The Sun Recorded Through History

## Scientific Data Extracted from Historical Documents

ASSL

# The Sun Recorded Through History

# Astrophysics and Space Science Library



For other titles published in the series, go to
http://www.springer.com/series/5664

# The Sun Recorded Through History

J. M. Vaquero
*Universidad Extremadura,*
*Cáceres*
*Spain*

and

M. Vázquez
*Instituto de Astrofísica de Canarias,*
*Tenerife*
*Spain*

Springer

José M. Vaquero
Universidad Extremadura
Departamento de Física Aplicada
Avenida de la Universidad, s/n
10071 Cáceres
Spain
jvaquero@unex.es

M. Vázquez
Instituto de Astrofísica de Canarias
c/ Vía Láctea s/n
38200 La Laguna
mva@iac.es

ISBN 978-0-387-92789-3 e-ISBN 978-0-387-92790-9
DOI 10.1007/978-0-387-92790-9
Springer Dordrecht Heidelberg London New York

Library of Congress Control Number: 2009921141



Printed on acid-free paper

Springer is part of Springer Science+Business Media (www.springer.com)

# Preface

The Sun is nowadays observed using different techniques that provide an almost instantaneous 3-D map of its structure. Of particular interest is the study of the variability in the solar output produced by the dissipation of magnetic energy on different spatial and temporal scales – the so-called magnetic activity. The 11-year cycle is the main feature describing this phenomenon. Apart from its intrinsic scientific interest, this topic is worth studying because of the interaction of such processes with the terrestrial environment. A fleet of space and ground-based observatories are currently monitoring the behaviour of our star on a daily basis.

However, solar activity varies not only on this decadal time-scale, as has been attested mainly through two methods: (a) records of the number of sunspots observed on the solar surface from 1610, and (b) the records of cosmogenic isotopes, such as $^{14}$C and $^{10}$Be, measured in tree-rings and ice-cores, respectively.

The study of the long-term behaviour of solar activity may be complemented by the study of historical accounts describing phenomena directly or indirectly related to solar activity. Numerous scientific and non-scientific documents have reported these events and we can make use of them as a proxy of solar activity in past times.

In this book we shall review these descriptions of solar activity in the past, providing, on the one hand, primary material for the history of astronomy and, on the other hand, verifying or rebuffing current ideas concerning the time variability of the Sun on the scale of centuries. We shall concentrate on documents that provide information on these topics before the discovery of photography around 1840. Modern drawings will also be included. The lower temporal limit of our study will be set by the archaeoastronomy of prehistoric sources.

The first chapter provides the necessary background on the Sun, with special emphasis on the observing techniques and the influences of the telescope and the Earth's atmosphere on the information obtained from solar observations. A list of books on solar physics is included at the end of this chapter.

Naked-eye observations offered the first possibility to distinguish certain structures, eventually called sunspots, on the apparently pure solar surface. In the second chapter we give an overview of these records and their adequacy to reveal long-term variations of solar activity.

The discovery of the telescope was a turning point in the history of science, with special impact on our knowledge of the Universe and, of course, of the Sun. For centuries the eye and the hand were combined by astronomers to produce excellent drawings of the observed solar structures, most of them on sunspots. This chapter summarizes the work of different solar astronomers until the invention of photography and its application to solar observations. These drawings can be used not only as a tool for informing us about the temporal variation of solar activity, but also to extract physical knowledge about the structures observed. The Wilson effect and the determination of solar rotation are two of these applications described at the end of the chapter.

Chapter 4 is dedicated to one of the most fascinating spectacles given by Nature, total solar eclipses. When the skies were clear, historical documents have always reported these phenomena. In the 18th century, the pioneering work of E. Halley made it possible to forecast solar eclipses with greater accuracy; this, together with the advances in navigation, enabled scientific expeditions to be carried out in order to observe these events.

Since the beginnings of astronomy, astronomers have tried to measure the relevant scales of our accessible vicinity, the Solar System. The development of trigonometry and the art of measuring small angles on the sky were essential tools for this purpose. In Chapter 5, we describe in some detail first the measurements of the solar diameter and then the transits of Mercury and Venus across the solar disk, a phenomenon that for centuries was essential to measuring the Earth–Sun distance. Nowadays, planetary transits in our Solar System are an excellent tool for calibrating current and future observations of exoplanets transiting the disk of other suns.

The mythology of several cultures of the people living in northern latitudes is connected with the aurorae, an event known to originate from transitory phenomena on the Sun. Step by step, the scientists brought this topic to the field of science, showing its relation with transitory events occurring on the solar atmosphere such as flares and coronal mass ejections.

The final aim of the present work is to complement previous studies on the reconstruction of solar activity in the past. The reference to the excellent work made by D.V. Hoyt and K.H. Schatten is our starting point. With this idea in mind, we summarize the available data in the last chapter, proposing tasks to be done in the future.

Many people have been involved, in different ways, in the preparation of this book. At the IAC, R. Castro elaborated and retouched a substantial number of the figures, and the Library staff (M. Gómez and L. Abellán) provided an excellent service in tracing old publications. Parts of this work were written at the CHCUL and IDL-CGUL (University of Lisbon, Portugal).

J.A. Bonet, J. Casanovas, M.C. Gallego, B. Ruiz Cobo, J. Sánchez Almeida, F. Sánchez Bajo, S. Sofia, R.M. Trigo, R. Vílchez Gómez and A. Wittmann have critically read different drafts of individual chapters of the book and gave valuable comments, advice and suggestions.

Figures, data and different suggestions have also been kindly supplied by A. Ardanuy, J.A. Bonet, P. Hingley, J.M. Pasachoff, Y.A. Nagovitsyn, P. Ribeiro, P. Rocher, F.R. Stephenson, I.G. Usoskin, E. Vázquez Dueñas, D.M. Willis, A. Wittmann and H. Wöhl. We would also like to thank the NASA ADS service, which provides a wonderfully efficient service to the scientific community.

Anna Fagan and Robert Chatwin helped to make this book readable in English. We alone, however, bear the responsibility for its content. We thank the Springer staff, especially Dr. Harry Blom, for his confidence in our work. We acknowledge the excellent work done by Lydia Shinoj and her team (Integra) during the production of the book.

Finally, our families showed great patience and gave us their full support during the lengthy process of writing this book, which we dedicate to our wives and children.

Badajoz and La Laguna — J.M. Vaquero
November 2008 — M. Vázquez

# Contents

# 1

# The Sun

Our Sun is an ordinary star of spectral type G2V. However, there are several reasons why its study deserves special attention. For example, it is the only star where we can directly observe details on its surface; this allows astronomers to test theories of great relevance. Let us mention only one of them: the identification of the process of nuclear fusion in its interior laid the foundation for discovering its age and for understanding the evolution of the stars. Another reason is that the Sun clearly influences the Earth's environment at different time scales, producing events that have impressed both astronomers and laymen alike. The latter aspect is the one we will be addressing in this book.

In this chapter we will provide the necessary background on the Sun for interpreting the knowledge hidden in the historical, scientific and non-scientific documents.

## 1.1 The Solar Structure

During the 19th century it became evident that the age of the Earth could be estimated as hundreds of millions of years. This stimulated research about possible energy sources that were able to keep the Sun shining for such a long period of time.

Basically, we can make a distinction between the interior of the Sun and its atmosphere. The Sun's interior can be further divided into the following layers, starting from the centre (see Table 1.1):

- *Core*: this is the region where nuclear fusion takes place. Hydrogen is converted into helium and, since the Sun is mainly composed of H and He, its nuclear fuel lasts for $10^{10}$ years in total. The temperature is about $1.5 \times 10^7$ K.
- *Radiative zone*: here the energy is transported outwards by radiation.

J.M. Vaquero, M. Vázquez, *The Sun Recorded Through History*,
Astrophysics and Space Science Library 361, DOI 10.1007/978-0-387-92790-9_1,

**Table 1.1.** Basic characteristics of the main zones of the solar interior. $\rho^1_{\mathrm{atm,SL}}$ is the density of the Earth's atmosphere at sea level. $R_\odot$ stands for the solar radius

| Name | Extension in $R_\odot$ | Temperature | Density [g/cm$^3$] |
|---|---|---|---|
| Core | 0–0.25 | $1.5 \times 10^7$–$7 \times 10^6$ | 150–20 |
| Radiative zone | 0.25–0.70 | $7 \times 10^6$–$2 \times 10^6$ | 20–0.2 |
| Tachocline | thin | | |
| Convective zone | 0.70–1.0 | $2 \times 10^6$–$7 \times 10^3$ | 0.2–$1/10000\rho^1_{\mathrm{atm,SL}}$ |

- *Tachocline*: in this thin zone, shearing motions occur between the fluid motions of the upper lying convection zone and the stable radiative zone; these motions are able to produce the magnetic fields that eventually emerge at the surface.
- *Convection zone*: because of the lower temperature, atoms become only partially ionized, which increases the opacity and gives rise to convective motions.

We will now briefly discuss the solar atmosphere from which the radiation originates.

The *photosphere* is a layer that is only about 400 km thick and where more than 90% of the solar radiation is emitted (especially in the visible). This layer is often referred to as the solar surface.

Above the photosphere the temperature rises from a minimum of about 4500 K to several $10^4$ K in the *chromosphere*. In the subsequent transition zone the temperature increases very sharply to several $10^5$ K, and the outermost layer of the solar atmosphere is called the *corona*. The chromosphere and the corona cannot be observed under normal conditions because these layers are very faint in comparison with the solar surface. The first observations of the corona were made during total solar eclipses. The temperature there is several $10^6$ K. In Table 1.2 and Figure 1.1 we give the basic parameters of these layers.

**Table 1.2.** Basic characteristics of the solar atmosphere

| Name | Extension | Temperature | Density [g cm$^{-3}$] |
|---|---|---|---|
| Photosphere | 400 km | 7000–4500 | $\sim 10^{-7}$ |
| Chromosphere | $\sim 10^4$ km | $10^4$ | $10^{-12}$ |
| Transition region | thin | | |
| Corona | $R_\odot$ | $10^6$ | $10^{-17}$ |

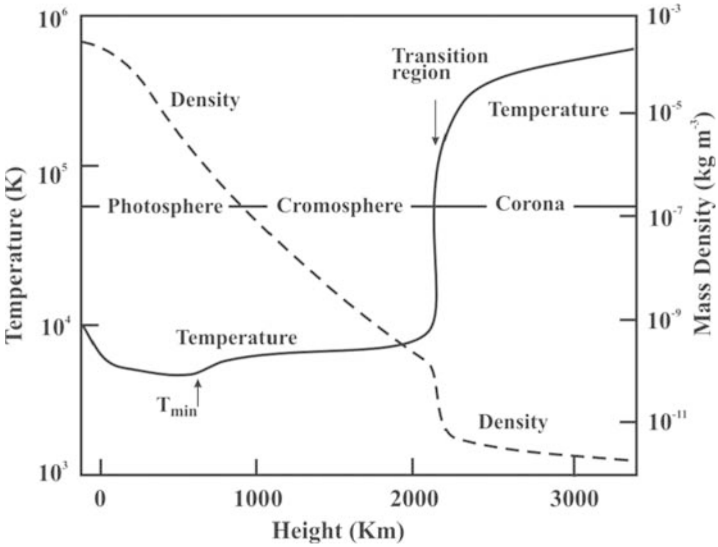


**Fig. 1.1.** Variation of temperature and density in the solar atmosphere. Adapted from Athay (1976).

## 1.2 The Photosphere

### 1.2.1 The Solar Spectrum

The mean temperature of the photosphere is 5770 K. According to this value, the Sun will emit most of the energy in the visible range. At a wavelength of 550 nm its flux outside the atmosphere is $1.96\,\mathrm{J\,m^{-2}\,s^{-1}}$, corresponding to a photon flux of $5.4 \times 10^{18}$ photons $\mathrm{m^{-2}\,nm^{-1}\,s^{-1}}$.

One of the primary objectives of early solar astrophysics was the measurement of the spectral distribution of solar irradiance. It soon became evident that the terrestrial atmosphere filters out an important part of the solar radiation (Figure 1.2). Table 1.3 summarizes the main atmospheric components contributing to this absorption.

The solar constant, S, is defined as the integrated solar spectral irradiance over all wavelengths. It is given in $\mathrm{Wm^{-2}}$ and corrected to 1 AU.[1] The derived value from daily averages from six satellites over 1978–1998 is $S = 1365.1\,\mathrm{Wm^{-2}}$ (Cox, 2000).

The prism experiment carried out by I. Newton in 1665 opened the possibility to study solar radiation in different colours. One bright sunny day, Newton darkened his room and made a hole in his window shutter, allowing just one beam of sunlight to enter the room. He then took a glass prism and placed it in the sunbeam. The result was a spectacular multicoloured band of

[1] 1 AU = 1 astronomical unit = mean Sun–Earth distance = 149 598 500 km.

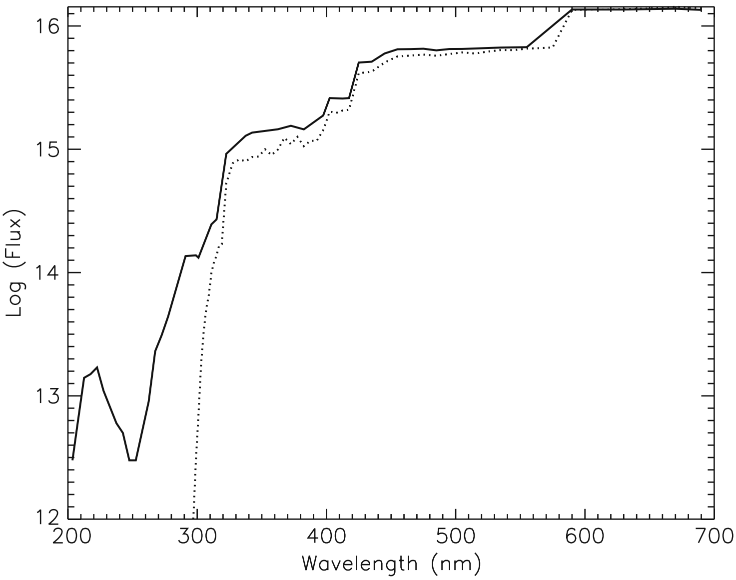


**Fig. 1.2.** The solar spectrum at an altitude of 40 km (solid line) compared with that recorded at the surface (dotted line).

light just like a rainbow, called a colour spectrum. In a second experiment, he placed another prism upside-down in the way of the light spectrum after passing through the first prism. The band of colours combined again into white sunlight. However, Newton thought that colour was not a physical property but a psychological phenomenon.

William Wollaston (1766–1828) in 1802 published a paper describing a solar spectrum and seven dark lines within it. The importance of these lines was not realized by Wollaston or his readers.[2] He used a slit one-twentieth of an inch wide, and viewed directly through a prism of flint glass held in front of his eye (Wollaston, 1802).

**Table 1.3.** Main components contributing to the absorption of radiation in the terrestrial atmosphere. Wavelengths are expressed in microns

| Absorbing Agent | Absorbing Window |
|---|---|
| Atomic oxygen, nitrogen | 0–0.085 (X - rays) |
| Molecular oxygen, nitrogen | 0.085–0.2 (Far UV) |
| Ozone ($O_3$) | 0.2–0.35 (Near UV) |
| $CO_2$, $CH_4$, $H_2O$, $NH_3$ | Infrared bands |

[2] Wollaston suggested that the lines were the edges of the primary colours.

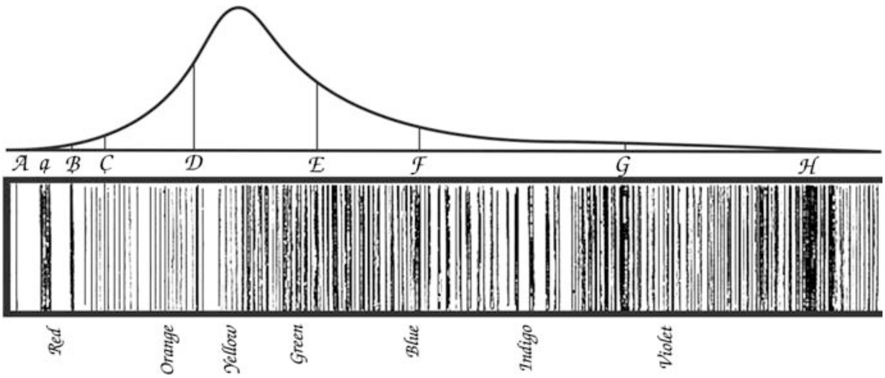


**Fig. 1.3.** Reproduction of Fraunhofer's original 1817 drawing of the solar spectrum. The more prominent dark lines are labelled alphabetically; some of this nomenclature has survived to this day. From Denkschriften der K. Acad. der Wissenschaften zu München 1814–15, pp. 193–226.

Joseph Fraunhofer (1787–1826) invented the spectroscope and the diffraction grating and in doing so transformed spectroscopy from a qualitative art to a quantitative science by demonstrating how one could measure the wavelength of light accurately. Examining the spectrum of solar light passing through a thin slit, he noticed a multitude (574) of dark lines (Figure 1.3).

The right interpretation of these dark features was done rapidly. John Herschel (1792–1871) demonstrated that when a substance is heated and its light passed through a spectroscope, each chemical element gave off its own set of characteristic bright lines of colour. The combined use of a prism and a narrow slit was the basic design of a spectrograph. The invention of the Bunsen burner, around 1850, and the development of the basic laws of radiation by Robert Kirchhoff (1824–1887) allowed the development of spectroscopy and the distinction between the different types of spectra (continuum, emission and absorption). Figure 1.4 shows one of the first spectroscopes built, by C.A. Steinheil (1801–1870) in Munich.

### 1.2.2 Limb Darkening and Optical Depth

A very well-known phenomenon on the Sun, visible with even small instruments, is limb darkening. The Sun appears brighter near the centre of its disk than near the limb. When we look at the centre of the solar disk in the visible range, near the centre we look into deep and hence hot regions (the temperature increases with depth). Towards the limb, we get radiation from higher and hence cooler levels (Figure 1.5). This is valid for the visible part of the solar spectrum.

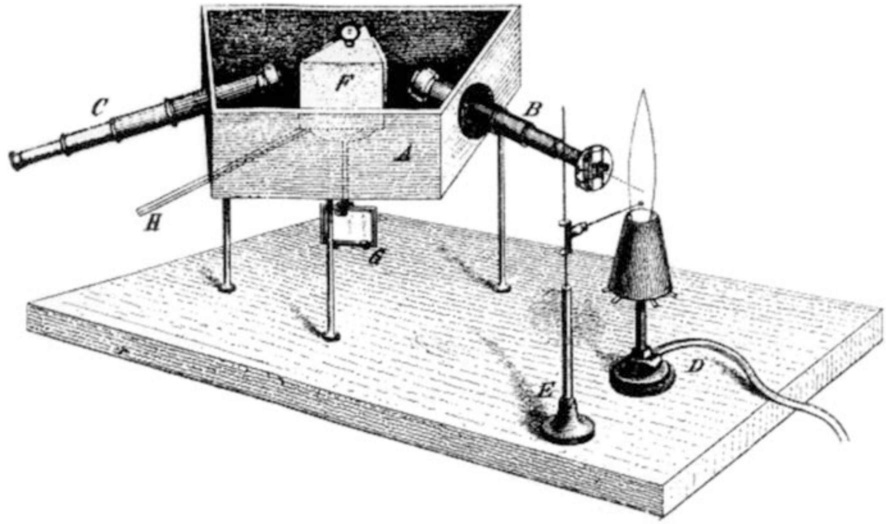


**Fig. 1.4.** One of the first spectroscopes. Adapted from Kirchhoff and Bunsen (1860).

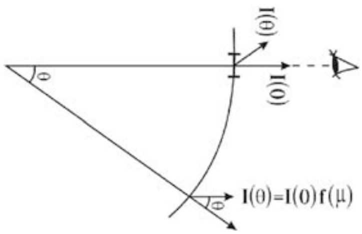


**Fig. 1.5.** The centre-to-limb variation of the photospheric brightness.

Elste and Gilliam (2007) describe different measurements of this parameter and the associated problems. The explanation of this effect lies in the interaction between the radiation and matter in the solar atmosphere.

The absorption coefficient, which determines how deep we see into the solar atmosphere, increases rapidly toward the blue part of the spectrum. This means that, in the UV, we see higher parts of the solar atmosphere. At observations below $\lambda = 150.0\,\mathrm{nm}$, limb darkening changes to limb brightening. This phenomenon can be interpreted as follows: At wavelengths shorter than 150 nm, we look into areas above the temperature minimum of the Sun, which occurs at a height of about 500 km above solar surface level (see Figure 1.1). In summary, limb darkening is mainly a geometrical effect, but the depth we are observing when we look at the Sun depends also on the properties of the solar material which absorb the radiation.

The optical depth, $\tau$, measures how opaque the solar matter is to radiation passing through it. It is measured along the vertical path, $dz$, and in stellar atmospheres is defined so that $\tau = 0$ at sufficiently large distances from the star:[3]

$$d\tau_\lambda = -\kappa_\lambda dz = -\kappa_\lambda \cos\theta dh$$

where $\kappa$ is the extinction coefficient which is wavelength dependent. The coefficient per particle has the units of a cross-section ($\mathrm{cm}^{-2}$); per unit of volume is $\mathrm{cm}^{-1}$ and per unit of mass $\mathrm{cm}^2/\mathrm{g}$.

The radiation received from the Sun can be expressed as an integral that adds up the contribution of the different photospheric layers

$$\mathrm{I} = \int_0^\infty \mathrm{B}(\tau)\mathrm{e}^{-\tau}\mathrm{d}\tau$$

with $B(\tau)$ the emission of the layer with optical depth $\tau$, usually approximated by the Planck function. From this expression one finds that layers with $\tau \sim 1$ are those contributing to most of the observed signal. When $\tau \gg 1$ (deep layers) then $e^{-\tau} \sim 0$ and no light emerges from these layers. From the Eddington–Barbier approximation, we have $I = B(\tau = \cos\theta)$, where $\theta$ is the heliocentric angle. Towards the limb we observe radiation from upper and cooler layers, producing the observed limb darkening.

The absorption spectral lines are formed above the continuum, at heights depending on the atomic transition involved and the physical parameters of the atmosphere.

### 1.2.3 Granulation

Under excellent observing conditions, the photosphere exhibits a cellular pattern, called granulation, the cells being about 1000 km in diameter and a lifetime of 5–10 minutes (Figure 1.6). Solar granulation is the visible manifestation of the convection zone that lies below the photosphere. Hot matter rises in the bright granules, cools and then descends in the intergranular lanes. Whereas the upflow is relatively smooth, the downflow is more turbulent and in the downflowing areas, turbulent motions occur that can induce shock waves that penetrate into the overlying chromosphere and contribute to its heating.

Granules show a broad range of sizes, with the small ones being more abundant than the larger ones. The contrast of the granulation is given by the standard deviation of the brightness fluctuations in a selected rectangular field.

$$\Delta\mathrm{I}_{\mathrm{rms}} = \sqrt{\frac{1}{NM}\sum_{n=1}^{N}\sum_{m=1}^{M}\left[\frac{I(n,m)}{\overline{I}} - 1\right]^2}$$

[3] Actually, the surface level is defined as $\tau_{500} = 1$ where the subscript refers to the wavelength at which $\tau$ is given (500 nm).

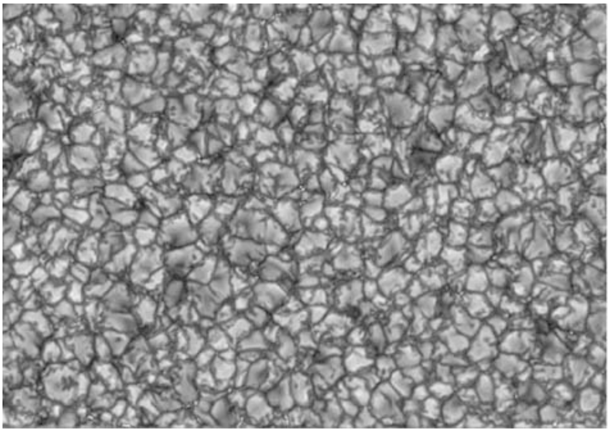

**Fig. 1.6.** Solar granulation observed in white light with the SST at the Roque de los Muchachos Observatory (La Palma). Courtesy: J.A. Bonet (IAC).

where $N$, $M$ are the dimensions of the granular field and $\overline{I}$ is its mean brightness. Values are wavelength-dependent with a maximum around 13% in the green.

Spectroscopic observations and theoretical development show that granulation is the upper manifestation of the solar convection zone. For monographs and reviews on solar granulation see Bray et al. (1984) and Muller (1999).

Solar convection is also present at other spatial and temporal scales. Supergranulation was first detected as a pattern in the velocity field and the typical cell size is about 30 000 km. In the centre, the upflow is about $50\,\mathrm{m\,s^{-1}}$, the downflow is about $100\,\mathrm{ms^{-1}}$; the lifetime of the supergranular cells is in the order of a day. For a general review on solar convection see Nordlund (2003).

### 1.2.4 Sunspots

#### General Characteristics

Sunspots are the oldest known direct manifestations of solar activity. Most consist of a central dark region, known as the umbra (temperature about 4000 K) and a surrounding less dark filamentary region, the penumbra (temperature about 5000 K). Sunspots without penumbra are usually called *pores*. The sunspots are darker than their surroundings because they emit less energy per unit area.

Sunspots appear in groups, and a morphological classification of their evolution in nine classes or steps was proposed by M. Waldmeier (1912–2000) at the Zürich Observatory (Figure 1.7) in 1938. This classification scheme delineates characteristic evolutionary stages of sunspot groups, though not all

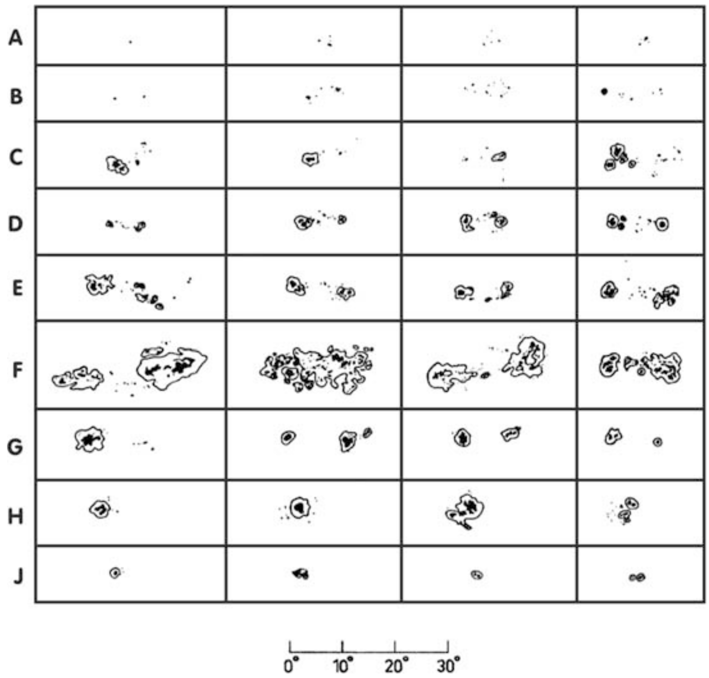


**Fig. 1.7.** The Zürich morphological classification.

groups go through each stage. Most groups go only part way through the steps and then either rapidly go backwards through the classes or decay to the final class.

### Areas and Lifetimes

Half of all sunspot groups have lifetimes, T, of less than two days, and only 10% last for more than 11 days. Waldmeier (1955) derived an empirical formula relating both parameters

$$T(\text{days}) = 0.1A_{\text{max}}$$

where $A_{\text{max}}$ is the maximum area expressed in millionths of solar hemisphere.

### Fine Structure

Very often the umbrae of individual sunspots within a group are divided into different parts by a bright structure known as a light-bridge (hereafter LB). We will call these individual umbrae "umbral cores" (UCs). A schematic view of the fine structures observed in sunspot umbrae is shown in Figure 1.8.

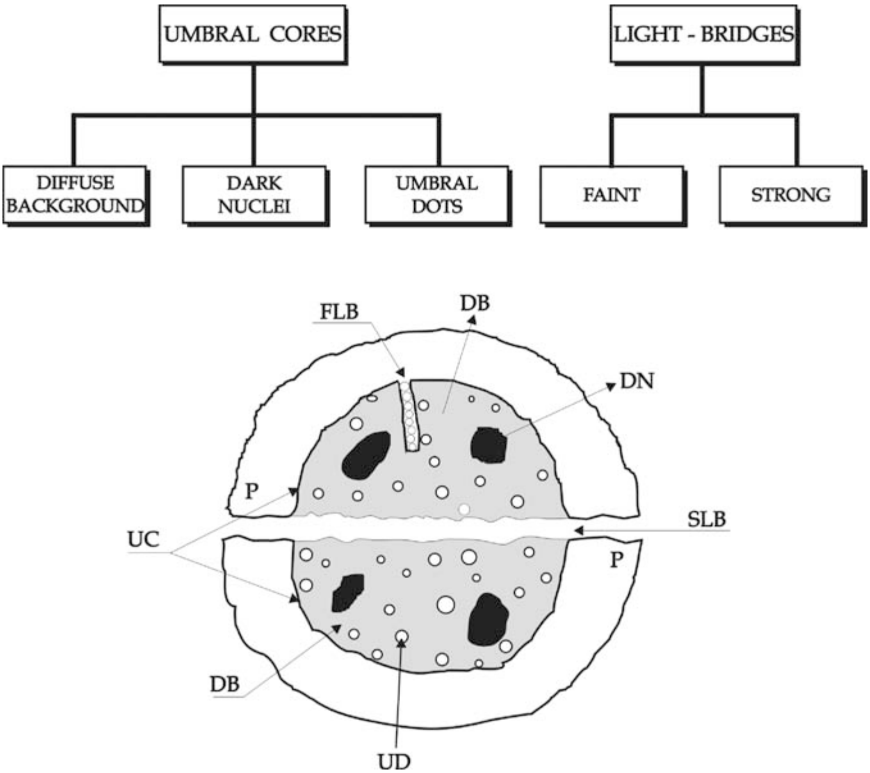


**Fig. 1.8.** An idealized scheme showing the different fine structures visible in sunspot umbrae. DN (Dark Nuclei), DB (Diffuse Background), UC (Umbral Core), FLB (Faint Light-Bridge) and SLB (Strong Light-Bridge).

Umbral cores have smoothly varying intensities with brighter and darker regions, known as the diffuse background (DB), which has two principal features, the dark nuclei (DN), which correspond to distinctive local intensity minima of the core, and umbral dots (UDs), small bright structures embedded in the diffuse background. Vázquez (1973) presented photographs of the granular structure of light-bridges and their role in sunspot dissolution, obtained with a 15 cm refractor. For modern studies on these structures see Sobotka et al. (1994) and Socas Navarro et al. (2004). Table 1.4 summarizes the main observed properties of umbral fine structures.

The penumbra occupies 85% of the total sunspot area and has on average 75% of the photospheric brightness. Morphologically, it is characterized by dark and bright filaments (see Figure 1.9). Inward proper motions have been observed in the bright elements of the inner penumbra, while in the outer penumbra the proper motions are outwards.

**Table 1.4.** Characteristics of the main fine structures observed in sunspots (excluding pores). For LBs the size and brightness correspond to the individual grains, and the lifetime to the whole structure. The brightnesses are wavelength-dependent and here are indicated as a fraction of the mean photospheric intensity in the green spectral range

| Structure | Size ($''$) | Brightness | Lifetime |
|---|---|---|---|
| SLB | 1.2 | 0.6–1.0 | days |
| FLB | 0.5 | 0.5–0.7 | |
| DN | 1.5 | 0.1–0.4 | days |
| UD | $< 0.60$ | 0.2–1.0 | minutes |

## Magnetic Field

The discovery of strong magnetic fields in sunspots by G.E. Hale in 1908 marked a decisive milestone in our understanding of these structures (see Del Toro Iniesta, 1996 for the historical background of this event). A longitudinal magnetic field, B, splits one spectral line at the wavelength $\lambda$ into two components separated by a distance, $\Delta\lambda_{\rm B}$. This is the Zeeman effect

$$\Delta\lambda_{\rm B} = 4.7 \times 10^{-13} {\rm g\,B}\,\lambda^2$$

where $g$ is the Landé factor describing the sensitivity of the spectral line to the magnetic splitting. Its values range between 0 and 3.

Sunspots appear on the solar surface in groups structured as magnetic bipoles. From the magnetic point of view, sunspot groups can be classified as: $\alpha$, where only a sunspot of one polarity is visible, $\beta$, and finally $\gamma$, complex

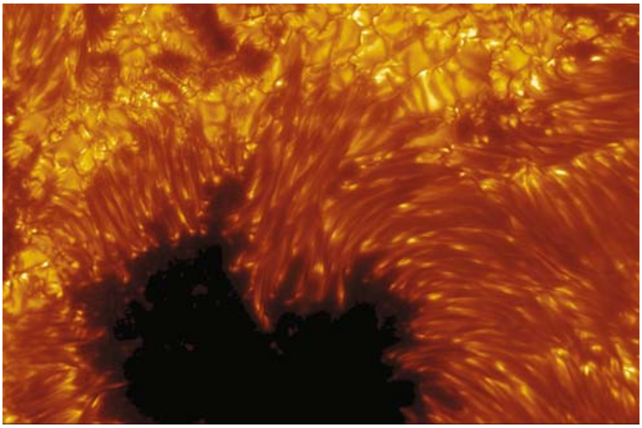

**Fig. 1.9.** A high-resolution picture of sunspot penumbra obtained at the 1 m Swedish Solar Telescope. Roque de los Muchachos Observatory (La Palma).

active regions in which the positive and negative polarities are so irregularly distributed as to prevent classification as a bipolar group.

*Individual spots*: The magnetic field strengths range from 1000 to 4000 gauss depending mainly on the sunspot size. It reaches peak values in the darkest part of the umbra where the field lines are generally close to the vertical. A clear correlation exists between magnetic field strength and temperature (Martínez Pillet and Vázquez, 1993).

At the penumbra, the mean field is inclined, becoming almost horizontal at the outer edge. It has long been a topic of debate whether the horizontal magnetic fied is concentrated in the dark or in the bright filaments. Recent measurements indicated a "corrugated" structure of the magnetic field. The magnetic field has an essentially horizontal component that carries the Evershed flow, and a less inclined component. The field strength is weaker where the fields are more horizontal (Thomas, 2000).

Biermann (1941) showed that the strong sunspot magnetic field would impede the convective motions carrying energy from the convective zone. In strong fields, matter can move only along the field lines, thus it is difficult for the material required for convective transport to return.

Parker (1979b) proposed that sunspot cores are composed of individual bundles of magnetic tubes. In order to hold the loose cluster of tubes together, a downdraft beneath the sunspot is needed. Local helioseismology support this hypothesis (Zhao et al., 2001).

Figure 1.10 shows a sketch of the structure of umbral dots within the cluster model. A hot plume of field-free gas penetrates from deep subphotospheric layers up to near the visible surface (shaded area).

Recent reviews on sunspots were given by Martínez Pillet (1997), Sobotka (1999) and Thomas and Weiss (2004).

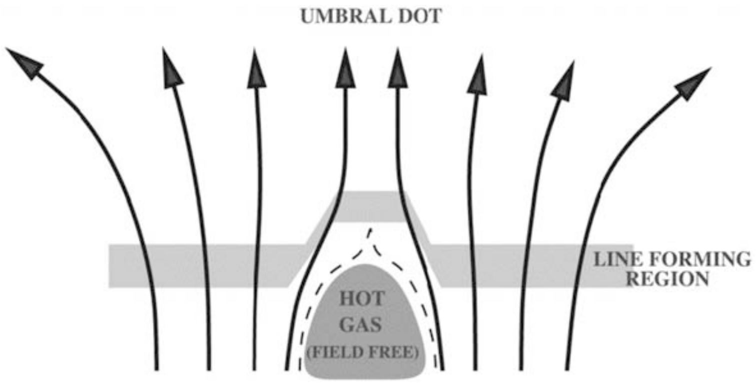


**Fig. 1.10.** Cartoon representation of an umbral dot in the sunspot cluster model. The solid lines with arrows represent magnetic field lines in the umbra. Adapted from Socas Navarro et al. (2004).

### 1.2.5 Faculae

Sunspots are usually accompanied by bright structures called faculae (see Figure 1.11). They often precede and considerably outlast the sunspots. The brightening in white light near the disk centre is barely detectable but increases towards the limb. Like sunspots, faculae are associated with strong magnetic fields.

The method of observing faculae near the disk centre is to use narrow-band filters centred on temperature-sensitive lines such as the CN-band at 384 nm (Sheeley, 1969) and the G-band[4] at 430.8 nm (Muller and Roudier, 1984). It was found that these bright structures correspond to small-scale concentrations of the magnetic field (Stenflo, 1966; Livingston and Harvey, 1969). In addition to these magnetic concentrations, there is a diffuse and complex magnetic field that pervades the whole solar photosphere. It is difficult to detect since it leaves almost no brightness signature in images, but it seems to contain a significant part of the solar magnetic flux (see e.g. Sánchez Almeida, 2004).

Table 1.5 shows the relevant parameters of the various magnetic structures observed in the solar photosphere.

A critical point is to understand how brightness is related to magnetic flux, going from bright faculae to dark sunspots. This phenomenon has been simulated numerically by Spruit and Zwaan (1981), who calculated the balance between the inhibition of convective energy transport (strong in large

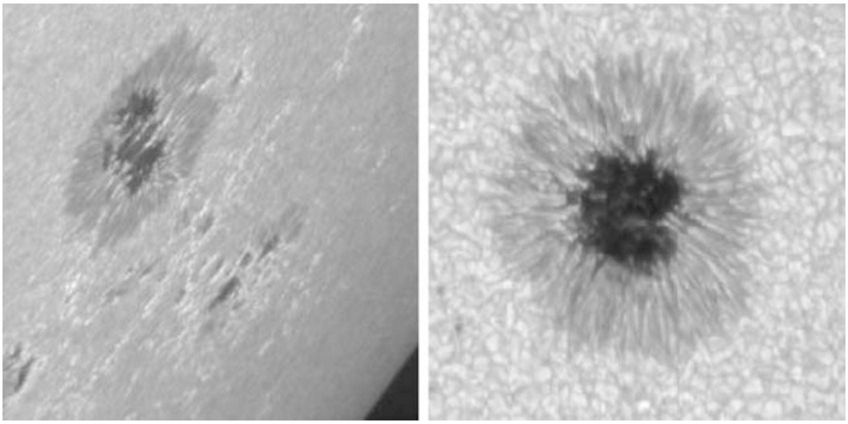

**Fig. 1.11.** Sunspots near the limb, where also faculae are seen (left) and near the disk centre where the surrounding granulation can be seen. (M. Sobotka, M. Vázquez, J.A. Bonet, A. Hanslmeier, 0.5 m Swedish Vacuum Solar Telescope, La Palma, Observatorio Roque de los Muchachos).

[4] It is called the G-band because it is the "G" feature of the original Fraunhofer spectrum shown in Figure 1.3.

**Table 1.5.** Hierarchy of magnetic concentrations in the solar photosphere. AR stands for Active Regions and QR for Quiet Regions. Adapted from Schrijver and Zwaan (2000)

| | Sunspots | Pores | Faculae | Quiet Sun |
|---|---|---|---|---|
| Flux ($10^{18}$ Mx) | $3\times10^4$–500 | 250–25 | $\leq 20$ | |
| Radius (Mm) | 28–4 | 1.8–0.7 | $\sim 0.1$ | |
| B (gauss) | 2900–2400 | 2200 | 1500 | 0–1500 |
| Cohesion | Compact | | In clusters | Very diffuse |
| Occurrence | Active Regions | | QR and AR | Everywhere |

magnetic concentrations and in deep layers) and lateral radiative heating from the non-magnetic surroundings, which is substantial in small magnetic structures having less density. They found that the transition between bright and dark structures occurs at sizes around 700 km. More recently, an intermediate family has been found, called dark faculae, which are dark in the centre of the solar disk and bright at the solar limb (see Figure 1.12).

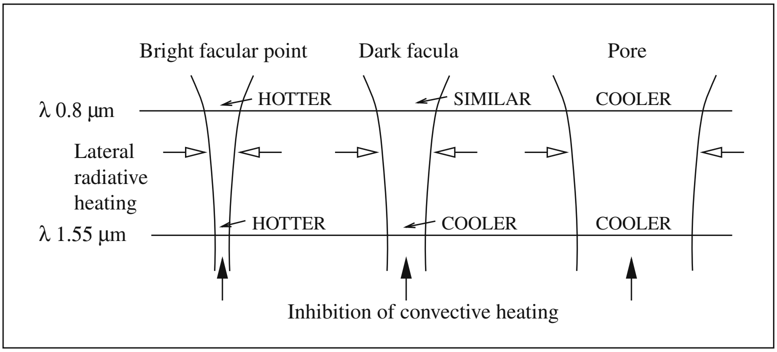


**Fig. 1.12.** Schematic view of temperature conditions in magnetic features of different sizes. Adapted from Sobotka et al. (2000). At 1.55 and 0.8 μm are located the minimum (deep layers) and the maximum (upper layers) of the absorption continuum coefficient of the solar atmosphere, respectively.

## 1.3 Observing the Solar Surface

Basic instructions to observe the solar surface are given in Beck et al. (1995), Kitchin (2002) and Macdonald (2003). More specialized monographs are Sánchez et al. (1992), Rimmele et al. (1999), Von der Lühe (2001) and Bhatnagar (2003).

### 1.3.1 Telescope Basics

A telescope is an instrument that gathers light coming from an object and focuses that light to build up an image. Basically, it consists of a convergent optical system, called the objective. The objective of diameter D forms the image of the object in the focal plane at a distance f (Figure 1.13). The f-ratio = f/D describes the performance of the telescope.

The diameter of the image of the full Sun in the prime focal plane is

$$d = 2\,fR_S/A$$

where $R_S$ is the solar radius and A the distance to the Sun. The resulting long focal distances is a major characteristic of many solar telescopes.

The subtended angle in radians is $\phi = d/f$, and since one radian is 206265 arcseconds, then the image scale (i.e. millimetres subtended by one arcsecond) is

$$s = \frac{f}{206265}$$

Many solar observations were done by the projection method, but soon a second convergent system of lenses, the eyepiece, was added, allowing the enlargement of the primary image of the object for a more detailed study. The angular magnification supplied by the eyepiece is

$$\text{Magnification} = \frac{\text{Focal length of the telescope}}{\text{Focal length of the eyepiece}}$$

If the eyepiece of a telescope is in the right place, the image is "in focus", and will appear sharp. To put the eyepiece in that position, the telescope has a mechanical device called the focuser, which allows you to shift the eyepiece back and forth very precisely, by means of either a couple of focusing knobs using an electric motor, or simply by turning the eyepiece.

The image that comes through the telescope, through the eyepiece and onto the surface of your eye, will appear as a sharply focused disk of light. That disk of light is known as the exit pupil, and its size will vary according to how much magnification the eyepiece/telescope combination is providing. The formula to work out the size of the exit pupil is:

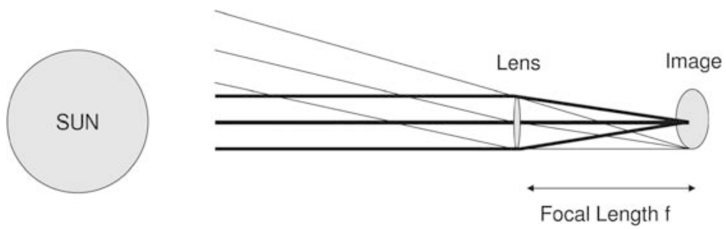


**Fig. 1.13.** Formation of a solar image by direct projection. Thick lines: rays coming from center of the solar disk. Thin lines: rays coming from the solar limb.

$$\text{Exit Pupil} = \frac{\text{D}}{\text{Magnification}}$$

Two main types of eyepieces have been used during the time covered by this book: (a) Huygens: designed by C. Huygens in 1703, consists of two plano-convex lens with the plane side towards the eye separated by an air gap. The main disadvantages are high image distortion and the narrow field of view. However, they can be very useful for solar projection. (b) Ramsden: designed by J. Ramsden (1735–1800) in 1783, comprises two plano-convex lenses of the same focal length and glass, placed less than one focal length apart. See Rudd (2007) for more details. The telescope field of view, FOV, is given by

$$\text{FOV} = \frac{\text{Eyepiece field of view}}{\text{Magnification}}$$

### 1.3.2 Image Formation of Extended Objects

Diffraction occurs because of the wave nature of light. The image of a point source is not a point but a disk surrounded by faint concentric rings (Figure 1.14), a pattern called the Airy disk. The size of the Airy disk expresses the maximum angular resolution of the optical system and is given by

$$\Delta\theta = \frac{r_1}{f} = \frac{1.22\,\lambda}{D}$$

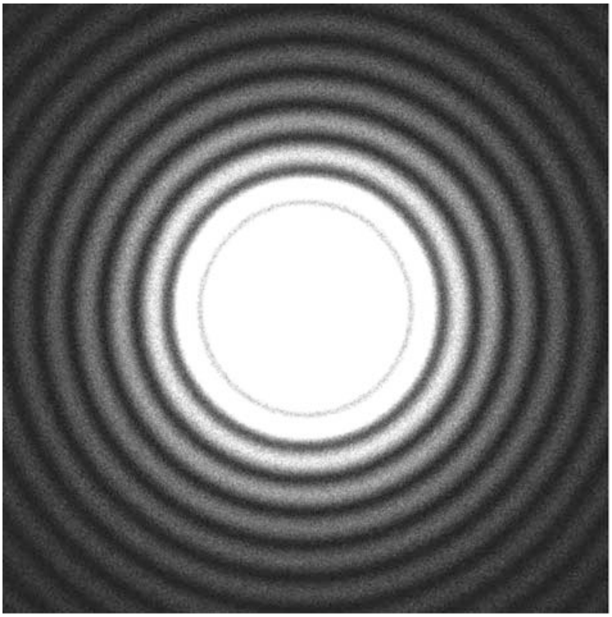

**Fig. 1.14.** Airy disk.

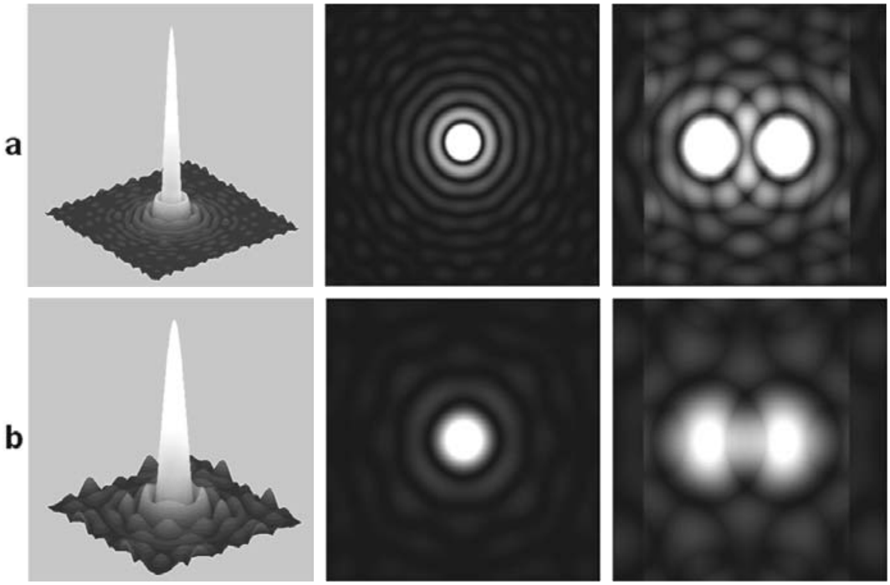


**Fig. 1.15.** Simulation of the image of a star. A larger telescope aperture (**a**) produces a concentration of light in a smaller space and therefore better spatial resolution. Two stars can be separated whereas with a smaller aperture (**b**) the two stars are seen as a blurred spot. Courtesy: A. Ardanuy (Astronomical Association of Sabadell).

where $r_1$ is the radius of the first dark Airy ring and $\Delta\theta$ the resolution in radians.

Figure 1.15 shows a simulation of the image of a star and its brightness distribution for two different telescope apertures.

The image of an extended object always suffers a certain degree of degradation when formed through an optical system such as a telescope. Let us imagine a simple case to illustrate how image degradation can be measured. We have as the object a sine wave grating formed by dark and light bars, separated by a distance $d$, the spatial wavelength (Figure 1.16).

Different parameters are used to describe the spacing of brightness in the objects and images. They are related by the following relations:

$$\mathrm{k} = \frac{\omega}{\mathrm{c}} = \frac{2\pi\nu}{\mathrm{c}} = \frac{2\pi}{\mathrm{d}}$$

where $k$ is the wavenumber, $\omega$ is the angular frequency (rad/sec), $\nu$ the spatial frequency and $c$ the speed of the propagation.

The modulation M of the light is measured by the function

$$\mathrm{M} = \frac{\mathrm{I_{max}} - \mathrm{I_{min}}}{\mathrm{I_{max}} + \mathrm{I_{min}}}$$